Conserved domains of human U4 snRNA required for snRNP and spliceosome assembly

Cornelia Wersig and Albrecht Bindereif
Max-Planck-Institut fuer Molekulare Genetik, Otto-Warburg-Laboratorium, Ihnestraße 73, D-1000 Berlin 33, FRG

Received August 13, 1990; Revised and Accepted September 20, 1990

ABSTRACT

U4 snRNA is phylogenetically highly conserved and organized in several domains. To determine the function of each of the domains of human U4 snRNA in the multi-step process of snRNP and spliceosome assembly, we used reconstitution procedures in combination with snRNA mutagenesis. The highly conserved 5′ terminal domain of U4 snRNA consists of the stem I and stem II regions that have been proposed to base pair with U6 snRNA, and the 5′ stem-loop structure. We found that each of these structural elements is essential for spliceosome assembly. However, only the stem II region is required for U4-U6 interaction, and none of these elements for Sm protein binding. In contrast, the 3′ terminal domain of U4 snRNA containing the Sm binding site is dispensable for both U4-U6 interaction and spliceosome assembly. Our results support an organization of the U4 snRNP into multiple functional domains, each of which acts at distinct stages of snRNP and spliceosome assembly.

INTRODUCTION

A prerequisite for the pre-mRNA splicing reaction is the assembly of splicing complexes consisting of small nuclear ribonucleoproteins and additional proteins (for a recent review, see 1). The spliceosome is assembled through a multi-step process that requires the coordinate interactions of U1, U2, U4/U6, and U5 snRNPs with the pre-mRNA, each other, and protein splicing factors. In contrast to U1 and U2 snRNPs, which contact the pre-mRNA directly (reviewed in 2), U4/U6 and U5 snRNPs appear to be bound in the spliceosome in a more indirect manner (3). Most likely, U4, U5, and U6 snRNAs enter the spliceosome in form of a U4/U5/U6 multi-snRNP (4,5,6), to which the separate U4/6 and U5 snRNPs associate through an ATP-dependent reaction (7). There is evidence that after spliceosome assembly a major conformational change weakens the binding of U4 snRNA (4,8,9) although U4 snRNA remains associated with the spliceosome through both steps of the splicing reaction (10). Thus it is apparent that of the spliceosomal snRNAs, U4, U5, and U6 snRNAs in particular engage in a multitude of interactions some of which may directly relate to the pre-mRNA splicing mechanism.

On the basis of a detailed phylogenetic study (11), an extensive base pairing interaction has been proposed to join together U4 and U6 snRNAs in the U4/U6 snRNP. Chemical cross-linking experiments (12,13,14) and a mutational analysis of the U4-U6 interaction (15) confirm this current secondary structure model (see also Figure 1). U4 snRNA can be divided into a 5′ terminal, a central, and a 3′ terminal domain (Figure 5). The 3′ terminal and central domains contain the Sm binding site flanked by two stem-loops; the phylogenetically strongly conserved 5′ terminal domain forms together with U6 snRNA a so-called Y structure organized in two U4-U6 intermolecular regions, stem I and stem II, separated by the intramolecular, 5′ terminal stem-loop structure of U4 snRNA.

In spite of a wealth of information on snRNA secondary structure and sequence conservation we know very little about U4/U6 snRNP proteins. U4 snRNA provides the Sm binding site for the common core proteins (B′BDD′EFG; reviewed in 16). So far no U4/U6 snRNP-specific proteins have been identified in mammalian cells (17). In contrast to the U4/U6 snRNP, the U5 snRNP has a very complex composition: 7 specific polypeptides in addition to the Sm protein complex were detected in the purified mammalian U5 snRNP (18).

Are U4 and U6 snRNAs held together only by base pairing; through what interactions do the U4/U6 and U5 snRNPs associate; and how is the U4/U5/U6 multi-snRNP complex integrated into the spliceosome? To address these questions and to delineate the functional domains of the human U4 snRNA, we are using *in vitro* snRNP reconstitution procedures in conjunction with U4 snRNA mutagenesis. We have previously reconstituted the U4/U6 snRNP in a functional form that assembles into splicing complexes (19) and used this approach to dissect the domain structure of human U6 snRNA (15). Here we demonstrate that the entire 3′ portion of human U4 snRNA including the Sm binding site is dispensable for spliceosome assembly. In contrast, all structural elements of the highly conserved 5′ terminal domain are essential for spliceosome assembly. Only the stem II region is required for U4-U6 interaction. In sum, these results support an assembly model whereby each of the structural elements of U4 snRNA functions at distinct stages of snRNP formation and spliceosome assembly.

MATERIALS AND METHODS

Plasmids and SP6 transcription

SP6-U4

The 0.7 kb EcoRI-HindIII fragment of p21 (20) containing the human U4C gene was purified, partially digested with AluI, and the AluI-AluI-HindIII fragment with most of the U4 sequence purified. Two oligonucleotides, 5'-GCGAATTCATTTAGGTG-ACACTATAG-3' and kinased 5'-CTTCTATAGTGTCACC-3' were hybridized, filled-in with the Klenow fragment of DNA polymerase, and cut with EcoRI. These two fragments were ligated into the EcoRI-HindIII vector fragment of pUC13. The expected sequence of the GpppG-capped SP6-U4 RNA after DraI run-off transcription is: GpppGA/AGCU...U4 coding sequence...ACUG/AAUUUUU (note that the boundaries between the natural U4 snRNA sequence and additional nucleotides of the synthetic RNA are indicated by /).

SP6-U4-EMBL8(+)

The EcoRI-HindIII-HindIII fragment of SP6-U4 containing the SP6 promoter and the human U4 sequences was subcloned into the EcoRI-HindIII vector fragment of pEMBL8(+).

SP6-U4ΔSm

SP6-U4 was cut with EcoRI and partially with HindIII. The EcoRI-HindIII-HindIII fragment containing the SP6 promoter and the U4 sequences was purified and recut with NlaIII. The 116bp EcoRI-NlaIII fragment with the SP6 promoter and partial U4 sequences was cloned into the EcoRI-SphI vector fragment of pEMBL130.

SP6-U4ΔStemI

SP6-U4ΔStemI corresponds to SP6-U4 with the stemI region (nucleotides 56−63 of U4 snRNA) deleted. SP6-U4ΔStemI was constructed by site-specific mutagenesis (21) using an oligonucleotide (5'-GGGGTATTGGGAAAAGTTTTCATAAT-CGCGCCTCGGATAAAACC-3') and SP6-U4-EMBL8(+).

SP6-U4ΔStemII

SP6-U4ΔStemII corresponds to SP6-U4 with the entire stem II region (nucleotides 1−16 of U4 snRNA) deleted. The expected 5' terminal sequence of the GpppG-capped SP6-U4ΔStemII-RNA is: GpppG/AGUAUC...(the boundaries between the natural U4 snRNA sequence and additional nucleotides of the synthetic RNA indicated by /). SP6-U4ΔStemII was constructed by PCR methodology. Using two oligonucleotides, 5'-GCGAATTCG-ATTTAGGTGACACTATAGAGTATCGTAGCCAATG-AGG-3' and the −48 reverse sequencing primer (5'-AGCGGATAACAATTTCACACAGGA-3', New England Biolabs), and SP6-U4 as a template, the mutant U4 fragment was amplified. It was cut with EcoRI and HindIII and cloned into the EcoRI-HindIII vector fragment of pEMBL8(+).

SP6-U4ΔStemII/2

SP6-U4ΔStemII/2 corresponds to SP6-U4 with the 5' half of the stem II region (nucleotides 1−8 of U4 snRNA) deleted. The expected 5' terminal sequence of the GpppG-capped SP6-U4ΔStemII/2-RNA is: Gppp/GCAGUG.... (the boundaries between the natural U4 snRNA sequence and additional nucleotides of the synthetic RNA indicated by /). SP6-U4ΔStemII/2 was constructed as SP6-U4ΔStemII, but using oligonucleotides 5'-GCGAATTCGATTTAGGTGACACTATA-GCAGTGGCAGTATCGTAGCCAATGAGG-3'and the −48 reverse sequencing primer (5'-AGCGGATAACAATTTCACA-CAGGA-3', New England Biolabs).

SP6-U4Δ5' stem-loop

SP6-U4Δ5' stem-loop corresponds to SP6-U4 with the 5' stem-loop region (nucleotides 19−55 of U4 snRNA) deleted so that there are two unpaired nucleotides left between stem I and stem II of each U4 and U6. The expected 5' terminal sequence of the GpppG-capped SP6-U4Δ5' stem-loop RNA is: GpppGA/AG CUUUGCGCAGUGGCAGUGCUAAUUGAAAA..... (note that the boundaries between the natural U4 snRNA sequence and additional nucleotides of the synthetic RNA indicated by /, the stem I and stem II regions by underlining). SP6-U4Δ5' stem-loop was constructed by site-specific mutagenesis (Kunkel, 1985) using the oligonucleotide 5'-GGGAAAAGTTTTCAATTAGC-ACTGCCACTGCGCAAAGC-3' and SP6-U4 EMBL8(+).

SP6 transcriptions of the DraI-cut SP6-U4, SP6-U4ΔStemI, SP6-U4ΔStemII, and SP6-U4ΔStemII/2 templates and of the XbaI-cut SP6-U4ΔSm were done as described (3). Biotinylated RNA was synthesized by including biotin-11-UTP (15 % of total UTP) in the transcription reaction. Other DNA templates have been previously described: SP6-U6 cut with BamHI (15) and MINX cut with BglI (22). All transcripts were capped with m^7GpppG.

Immunoprecipitation analysis

High-specific activity ^{32}P-labeled SP6-U4 RNA and mutant derivatives were reconstituted *in vitro* to snRNPs in a reaction containing 60 % DE53 reconstitution extract (19), 3.2 mM $MgCl_2$, 0.5 mM ATP, 20 mM creatine phosphate, 1.6 U/μl RNasIn, ^{32}P-labeled SP6-U4 RNA or mutant derivatives (5 ng/25 μl reaction), and tRNA (400 μg/ml). The reconstitution reaction was incubated at 30°C for 20 min and then at 37°C for 10 min. Of the total reconstitution reaction, 10% was used for RNA analysis (Total RNA, T lanes, Figure 2), the rest for anti-Sm immunoprecipitation (23). The immunoprecipitation efficiency was quantitated by Cerenkov counting of the RNA samples before gel electrophoresis.

Analysis of U4-U6 interaction

High-specific activity ^{32}P-labeled SP6-U4 RNA and mutant derivatives (200 ng/ml) were reconstituted *in vitro* to snRNPs as described above (immunoprecipitation analysis) except that unlabeled biotinylated SP6-U6 RNA was added (2 μg/ml). The 25 μl-reaction was filled up to 250 μl with washing buffer (20 mM Tris-HCl, pH 7.6, 400 mM KCl. 0.01 % Nonidet P40, 0.02 % sodium azide). Insoluble complexes were pelleted at 12,000 ×g for 2 min at 4°C, and to the supernatant 50 μl of a 1:1-suspension of preblocked streptavidin agarose (BRL; Ref. 24) was added. Affinity selection of U4/U6 complexes was carried out at 4°C for 60 min with gentle agitation. After pelleting, the streptavidin agarose beads were washed three times with 1 ml each of NET-2 buffer (50 mM Tris-HCl, pH 7.9, 0.5 mM DTT, 0.05 % Nonidet P40). Labeled U4 RNAs were purified by a proteinase K treatment at 55°C, phenol/chloroform extraction, and ethanol precipitation, and analyzed on 8 % denaturing polyacrylamide gels (pelleted RNA, P lanes, Figure 2). To compare the efficiencies of wild-type SP6-U4 and mutant derivatives to form U4/U6 complexes, one tenth of the total reaction was analyzed in parallel (total RNA, T lanes, Figure 2). The efficiency of U4-U6 interaction was quantitated by Cerenkov counting of the RNA samples before gel electrophoresis.

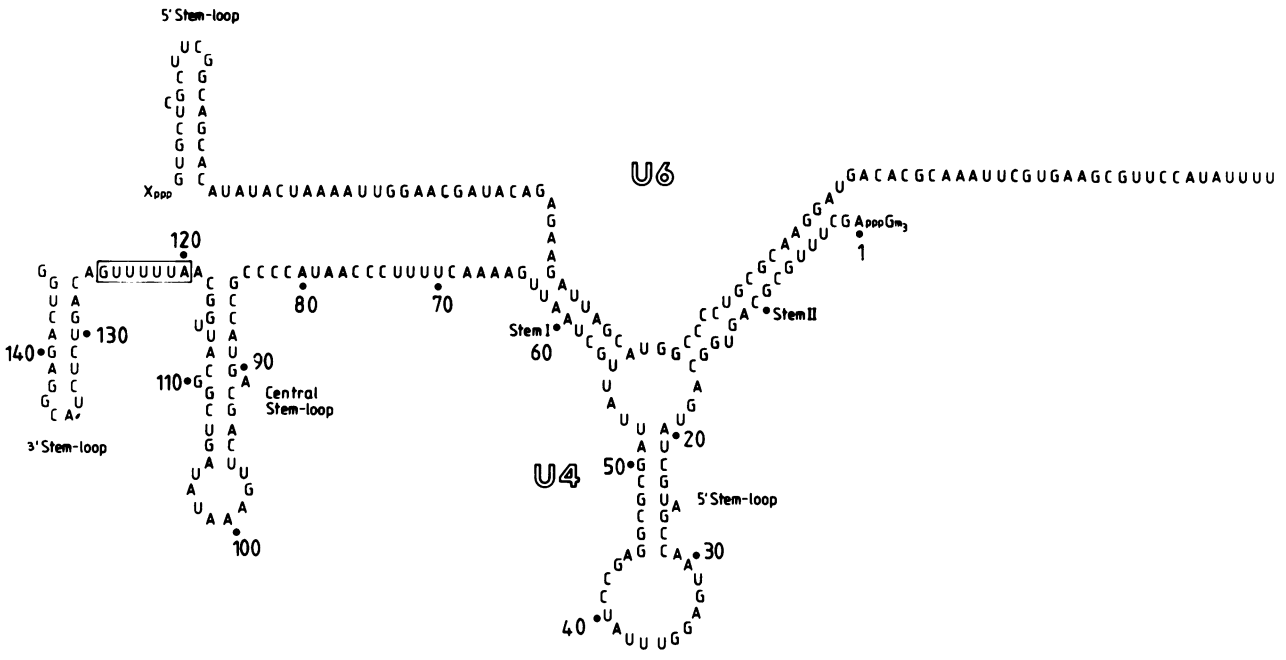

Figure 1. Secondary structure model of the human U4/U6 snRNP. This model corresponds to the U4/U6 consensus secondary structure (11). The Sm binding site of U4 snRNA is indicated by the boxed sequence. The human U4 and U6 sequences are taken from refs. 20 and 40, respectively.

Analysis of spliceosome assembly

High specific activity ^{32}P-labeled SP6-U4 RNA and mutant derivatives (300 ng RNA; ca. 10^7 cpm/μg) and unlabeled SP6-U6 RNA (900 ng) were reconstituted in a 125 μl-reaction to U4/U6 snRNPs as described above (immunoprecipitation analysis). The reaction was diluted with one volume of buffer (10 mM HEPES, pH 8.0, 3 mM MgCl) and KCl added to 100 mM. Reconstituted snRNPs were concentrated by pelleting in a Beckman TL-100 table-top ultracentrifuge (TL-100−2 rotor, 95,000 r.p.m., 2 hrs, 4°C). The pellet was dissolved in 15 μl buffer D and mixed with an equal volume of nuclear extract (25). Using this mixture at 60% and unlabeled MINX pre-mRNA (200 ng/25 μl reaction), splicing complexes were formed for 40 min under the conditions of *in vitro* pre-mRNA splicing (26,27). After the addition of heparin to 1 mg/ml, the splicing reaction was diluted with one volume of buffer (60 mM KCl, 20 mM HEPES, pH8.0, 1 mM $MgCl_2$) and applied on a 1 ml gradient (10−30 % glycerol in the same buffer. Glycerol gradient sedimentation was carried out in a Beckman TL-100 table-top ultracentrifuge (TLS 55 rotor, 55.000 r.p.m, 70 min, 4°C). The glycerol gradient was collected in 100 μl fractions from the top, and 40 μl aliquots of each fraction were analyzed by native RNP gel electrophoresis as described (28,29).

RESULTS

Mutational analysis of U4 and U4/U6 snRNP formation

To map U4 snRNA sequences required at the multiple stages of snRNP and spliceosome assembly we constructed a series of U4 derivatives (for a summary, see Figure 5). These U4 derivatives are deleted in RNA regions that form structural elements in the proposed secondary structure model (30). SP6-U4ΔSm lacks the Sm binding site and the flanking central and 3′ stem-loops. The deleted portion corresponds to the entire 3′ terminal and part of the central domain (nucleotides 91−145, Figure 1). A number of deletion derivatives are missing structural elements of the 5′ terminal domain: SP6-U4ΔstemI (nucleotides 56−63), SP6-U4ΔstemII (nucleotides 1−16), and SP6-U4ΔstemII/2 (nucleotides 1−8) are missing parts of the U4 region proposed to base pair with U6 snRNA; in SP6-U4Δ5′ stem-loop the 5′ stem-loop structure (nucleotides 19−55) is deleted (Figure 1).

Two assays were used to determine the reconstitution properties of U4 derivatives. First, by immunoprecipitation with anti-Sm antibodies we tested the U4 derivatives for the formation of the Sm core structure common to all spliceosomal snRNPs. Second, to determine the ability of U4 derivatives to interact with U6 snRNA, we devised a new assay. ^{32}P-labeled U4 derivatives are incubated under reconstitution conditions in the presence of biotinylated U6 snRNA. RNAs associated with U6 snRNA are then affinity-selected with streptavidin agarose, released by a heat treatment, and analyzed. The advantage of this assay lies in that it determines under these conditions the stability of the U4-U6 interaction and does not depend on the formation of a stable snRNP particle.

Figure 2 shows that wild-type U4 snRNA (SP6-U4) and all derivatives with deletions in the 5′ terminal domain (SP6-U4ΔstemI, SP6-U4ΔstemII, SP6-U4ΔstemII/2, SP6-U4Δ5′ stem-loop) are stable under the conditions of *in vitro* reconstitution and bind Sm proteins with similar efficiencies. In contrast, the U4 derivative with a deletion of the entire 3′ terminal domain including the Sm site (SP6-U4ΔSm), although stable under these conditions, did not reconstitute into a particle immunoprecipitable with anti-Sm antibodies. These data indicate that only the 3′ terminal domain with the Sm binding site and none of the structural elements of the 5′ terminal domain is essential for the association of Sm proteins with U4 snRNA.

To determine which U4 sequences are required for U4-U6 interaction, we tested wild-type U4 snRNA (SP6-U4) and all of our U4 derivatives for U4-U6 interaction under reconstitution conditions (Figure 3; compare 10% of total, lane T, with bound

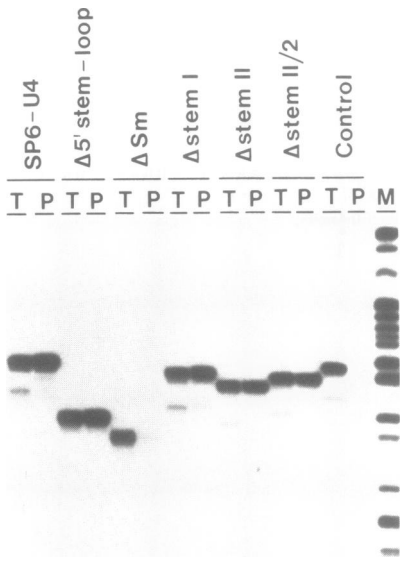

Figure 2. Analysis of reconstituted snRNPs by anti-Sm immunoprecipitation. ^{32}P-labeled SP6-U4 RNA and derivatives were reconstituted to snRNPs and assayed by anti-Sm immunoprecipitation as described in Materials and Methods. For each U4 derivative 10% of the total reconstitution reaction (total RNA, lane T) and the anti-Sm immunoprecipitated RNA (pellet, lane P) are shown. In a control reaction, non-immune human serum and wild-type SP6-U4 are used (control lanes). M, ^{32}P-labeled pBR322/HpaII marker fragments.

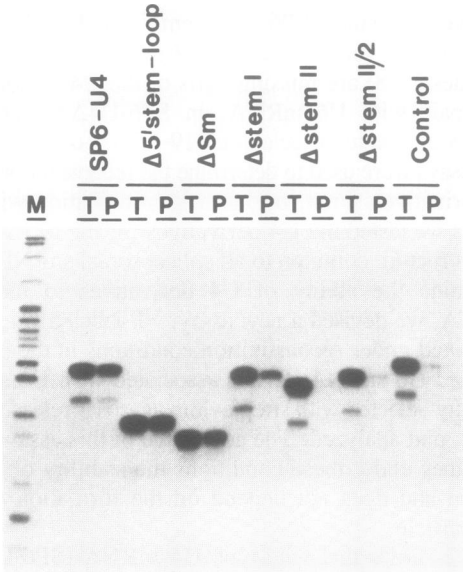

Figure 3. Analysis of the U4-U6 interaction. ^{32}P-labeled SP6-U4 RNA and derivatives were reconstituted in the presence of biotinylated, unlabeled SP6-U6 RNA. U4-U6 interaction was assayed by affinity selection with streptavidin agarose followed by the release of bound material. For each U4 derivative 10% of the total reconstitution reaction (total RNA, lane T) and all of the bound material (pellet, lane P) are shown. In a control reaction, unbiotinylated SP6-U6 RNA and wild-type SP6-U4 RNA were used (lane control). M, ^{32}P-labeled pBR322/HpaII marker fragments.

pelleted material, lane P). The efficiency of U4-U6 interaction under these assay conditions is for wild-type U4 snRNA approximately 10 % (Figure 3, lane SP6-U4). No RNA could be detected if unbiotinylated U6 RNA was used (Figure 3, lane control). Surprisingly, the Sm deletion derivative of U4 snRNA (SP6-U4ΔSm), which was unable to assemble an Sm core complex (see Figure 2), still associated with U6 snRNA at wild-type efficiency (Figure 3, lane vSm). However, deletions within the 5′ terminal domain behaved differently in U4-U6 interaction: Deleting the stem I of U4 snRNA reduced the ability to interact with U6 snRNA by about 50 % (Figure 3, lane ΔstemI), and deleting the stem II (lane ΔstemII) or part of stem II (lane ΔstemII/2) completely abolished the U4-U6 interaction; in contrast, deleting the 5′ stem-loop structure (lane v5′ stem-loop) reproducibly enhanced the U4-U6 interaction at least twofold.

These results regarding the U4-U6 interaction agree with the current secondary structure model of how U4 and U6 snRNAs interact to form the so-called Y structure (30). Both stem I and stem II are required for efficient U4-U6 interaction. In addition, our data indicate that the stem I and stem II regions may play different roles in the U4-U6 base pairing interaction and that this interaction is also influenced by the intramolecular 5′ stem-loop structure of U4 snRNA.

The Sm domain of U4 snRNA is dispensable for spliceosome assembly

The unexpected result that a U4 derivative lacking a functional Sm binding site still efficiently associates with U6 snRNA (Figure 3; SP6-U6vSm) raised the question whether this mutant U4 snRNA proceeds through the subsequent steps of snRNP and spliceosome assembly. To demonstrate assembly of reconstituted mutant U4 snRNPs into splicing complexes we used an assay system previously developed to show functional reconstitution of wild-type U4/U6 snRNP (19). ^{32}P-labeled wild-type and mutant U4 snRNAs are reconstituted with SP6-U6 RNA and incubated with an unlabeled pre-mRNA substrate under the conditions of the *in vitro* pre-mRNA splicing reaction. Splicing complexes formed with reconstituted, ^{32}P-labeled snRNAs are then analyzed by native RNP gel electrophoresis (28). Detection of ^{32}P-labeled U4 snRNA in the B complex indicates functional spliceosome assembly with reconstituted snRNPs. To overcome difficulties of resolving B complexes from large, non-specific U4 snRNA complexes (data not shown) and to improve the sensitivity of this assay we fractionated the crude splicing reaction by glycerol gradient sedimentation before RNP gel analysis. In addition, the sedimentation behaviour provides a further criterion that complexes formed with reconstituted, ^{32}P-labeled snRNAs represent B splicing complexes. Glycerol gradient sedimentation clearly resolves the A and B complexes from each other (Figure 4A, fractions 4−6 and 6−8, respectively) and from the very abundant non-specific U4 snRNA complexes (Figure 4B-G, fractions 1−4). The slightly slower electrophoretic mobility of the A complex in the first three fractions is probably caused by the relatively high protein concentration near the top of the gradient (Figure 4A, compare total reaction with fractions 1−3).

Wild-type U4 snRNA (SP6-U4), when reconstituted and assembled into splicing complexes *in vitro*, was clearly detected at the characteristic position of the B splicing complex (Figure 4B, fractions 6−8). The appearance of this complex depended on the addition of pre-mRNA substrate during spliceosome assembly (Figure 4C). Additional criteria for a complex of this electrophoretic mobility representing the B complex have previously been reported (19). When we analyzed the Sm deletion derivative (SP6-U4ΔDSm), we found to our surprise that it was incorporated into B splicing complexes, although at lower efficiency than wild-type U4 snRNA (Figure 4C, fractions 6−8). The lack of the core structure of U4 snRNP appears not to alter

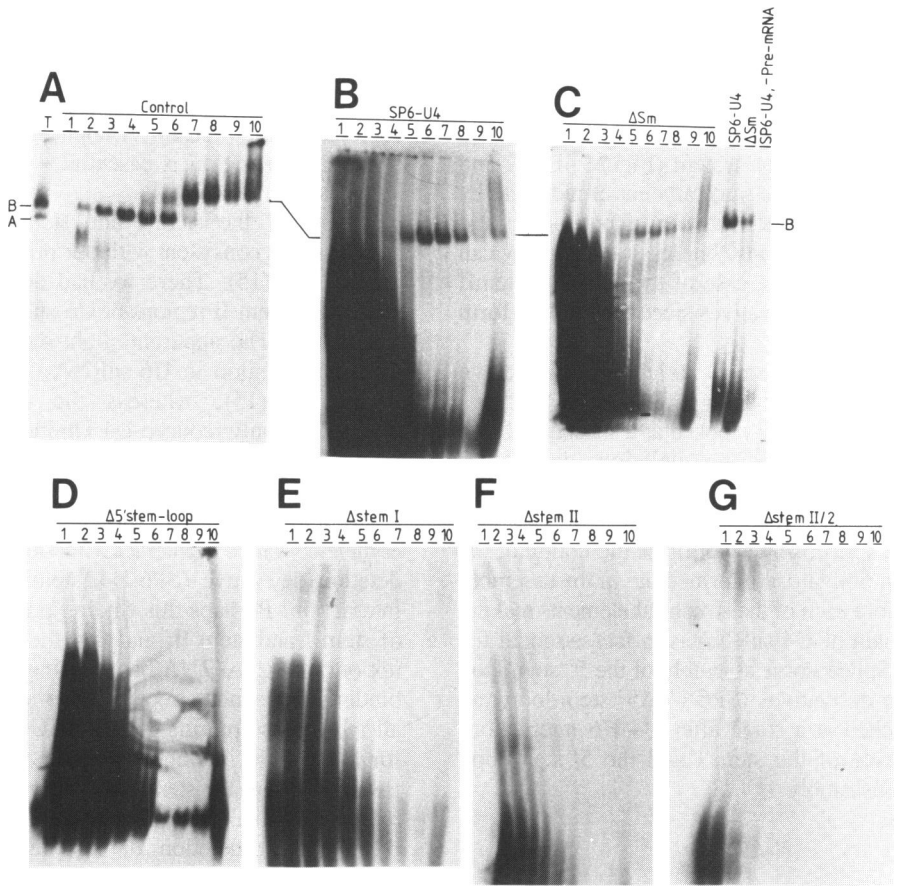

Figure 4. Analysis of spliceosome assembly. ^{32}P-labeled SP6-U4 RNA and derivatives were reconstituted in the presence of unlabeled SP6-U6 RNA. Reconstituted U4/U6 snRNPs were concentrated, added back to nuclear extract, and in the presence of unlabeled pre-mRNA under splicing conditions assembled to splicing complexes. This reaction mixture was then fractionated by glycerol gradient sedimentation and the gradient fractions analyzed by native RNP gel electrophoresis. As a control for the fractionation of splicing complexes and to obtain a marker position for the B splicing complex, a splicing reaction containing ^{32}P-labeled pre-mRNA was fractionated by sedimentation and RNP gel electrophoresis (Panel **A**; total reaction, lane T; gradient fractions #1–10, lanes 1–10). Panels **B-G** show the fractionation of splicing reactions containing reconstituted, ^{32}P-labeled snRNPs (SP6-U4 wild-type, panel **B**; SP6-U4ΔSm, panel **C**; SP6-U4Δ5′ stem-loop, panel **D**; SP6-U4Δstem I, panel **E**; SP6-U4Δstem II, panel **F**; SP6-U4Δstem II/2, panel **G**). The RNP gels shown in Panels B-G were run under identical conditions using a splicing reaction with ^{32}P-labeled pre-mRNA as a marker for the B complex (not shown). The electrophoretic positions of A and B complexes in the RNP gel are indicated. To the right of panel **C**, the respective gradient fractions #7 of splicing reactions containing ^{32}P-labeled SP6-U4, SP6-U4ΔSm, and SP6-U4 in the absence of added pre-mRNA are shown.

significantly the mobility of the resulting spliceosome in this native RNP gel system nor its sedimentation behaviour in glycerol gradients (compare Figure 4B and C). In sum, we conclude that the entire 3′ terminal domain of U4 snRNA including the Sm binding site has no essential function in spliceosome assembly.

Structural elements of the 5′ terminal domain of U4 snRNA are essential for spliceosome assembly

Next we asked whether any structural elements located within the 5′ terminal domain have essential functions during spliceosome assembly. The U4 snRNA derivatives carrying deletions within the 5′ terminal domain and described above (SP6-U4ΔstemI, SP6-U4ΔstemII, SP6-U4ΔstemII/2, and SP6-U4Δ5′ stem-loop; see Figure 5 for a summary) were reconstituted with SP6-U6 RNA and assembled into spliceosomes (Figure 4D–G). Figure 4D shows that the U4 derivative with a deletion of the 5′ stem-loop region (SP6-U4Δ5′ stem-loop) was not assembled into spliceosomes. Since this deletion resulted in an enhanced U4-U6 interaction (see Figure 3), we conclude that the 5′ stem-loop region is in fact essential for spliceosome assembly, at a stage subsequent to U4/U6 snRNP formation.

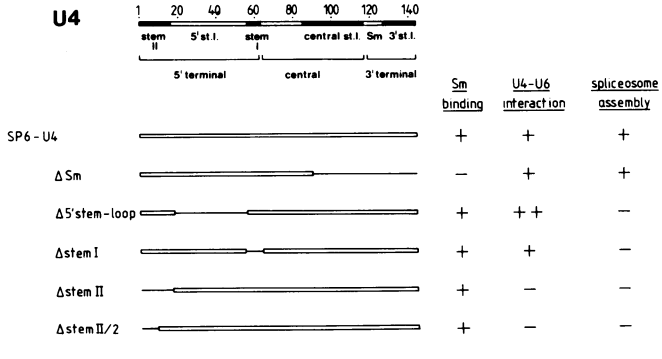

Figure 5. Organization of the U4 snRNA domain structure. The division of U4 snRNA in 5′ terminal, central, and 3′ terminal domains is schematically outlined as proposed by ref. 11. Below, the U4 RNA derivatives are schematically represented with the deleted regions indicated by thin lines. To the right, the ability of the U4 RNA derivatives to bind Sm proteins and to interact with U6 RNA is summarized (+, wild-type efficiency; ++, efficiency above wild-type levels; −, undetectable level; see Figures 2 and 3). The ability of the U4 RNA derivatives to assemble to spliceosomes is indicated as well (+, detectable; −, undetectable spliceosome assembly; see Figure 4).

The 5′ stem-loop region separates two regions of U4 snRNA, stem I and stem II, that form U4-U6 intermolecular helices in the proposed secondary structure model (30). None of the U4 derivatives with stem I and stem II deletions (SP6-U4ΔstemI, SP6-U4ΔstemII, and SP6-U4ΔstemII/2) resulted in detectable spliceosome assembly in our assay system (Figure 4E, F, and G, respectively). Approximately the same amount of radioactivity was used in each of these reconstitution experiments and fractionated on the glycerol gradients, but less radioactivity can be detected on the RNP gels in the case of the SP6-U4ΔstemII and SP6-U4ΔstemII/2 mutant derivatives since they do not form a U4/U6 snRNP.

We conclude that the stem I deletion derivative (SP6-U4ΔstemI), although still forming a U4/U6 snRNP (see Figure 3), appears to be completely blocked at a subsequent step of assembly to spliceosomes. The deletion derivatives SP6-U4ΔstemII and SP6-U4ΔstemII/2 have previously been shown to be deficient in U4-U6 interaction (see Figure 3). That they do not assemble to spliceosomes confirms the notion of the U4/U6 snRNP being an obligatory intermediate in the assembly of spliceosomes. Therefore each of the structural elements making up the 5′ terminal domain of U4 snRNA is in fact essential for spliceosome assembly. Spliceosome assembly of the 5′ stem-loop and the stem I deletion derivatives (SP6-U4Δ5′ stem-loop and SP6-U4ΔstemI) is blocked at a stage after U4-U6 interaction, suggesting a specific role of the stem I and the 5′ stem-loop region in spliceosome assembly.

DISCUSSION

We have applied an *in vitro* reconstitution approach in combination with a mutational analysis to delineate functional domains of human U4 snRNA. Such an approach opens up the possibility to investigate biochemically the snRNA functions at each of the multiple steps of snRNP and spliceosome assembly and splicing. In contrast to *in vivo* studies, functional reconstitution of snRNPs does not require steps such as snRNA processing or snRNP transport. Since there is currently no mammalian system available to study the splicing function of reconstituted snRNPs, we restricted our analysis to the snRNP assembly steps leading to the incorporation of snRNPs into the spliceosome.

Studying snRNA deletion derivatives through reconstitution led us to the conclusion that individual structural elements of U4 snRNA play distinct roles in the assembly pathway. In summary, our results in conjunction with earlier studies on the function of the Sm binding site (see below) suggest that the U4 snRNA molecule can be divided into two functional halves: The 3′ terminal and central domain containing the Sm binding site with snRNA maturation and snRNP transport functions, and the 5′ terminal domain with U4-U6 interaction and spliceosome assembly functions.

First, we found that the entire 3′ terminal and part of the central domain containing the Sm binding site (AU_5G, nucleotides 119−125; see Figure 1) are dispensable for U4-U6 interaction and spliceosome assembly. Earlier studies on the U2 snRNP had demonstrated that the Sm binding site is required for cytoplasmic cap trimethylation and cytoplasmic-nuclear snRNP transport (31,32). The Sm binding site of the U4/U6 snRNP, which U4 snRNA provides, may perform an analogous function. In addition, for both the U1 snRNP (33,34) and the U2 snRNP (31) a stabilizing function of the Sm proteins on the binding of specific snRNP proteins has been suggested. Similar reasons may cause the reduced efficiency of the Sm deletion derivative (SP6-U4ΔSm) in spliceosome assembly.

Second, our reconstitution studies suggest a functional subdivision of the 5′ terminal domain. The stem I and stem II regions are required for efficient U4-U6 interaction, whilst the 5′ stem-loop region is essential only at a subsequent stage of spliceosome assembly.

A role of the stem I and stem II regions in the U4-U6 interaction is consistent with our previous mutational analysis of U6 snRNA (15). There we had demonstrated that both intact stem I and stem II regions of U6 snRNA are required for U4-U6 interaction. The apparent slight discrepancy that a deletion of the stem I region in U6 snRNA completely abolished U4-U6 interaction (15), whereas the corresponding deletion in U4 snRNA only reduced U4-U6 interaction (this study), is most likely caused by the use of different assay conditions (data not shown). It is somewhat surprising, however, that both stem II deletion derivatives (SP6-U4ΔstemII and SP6-U4ΔstemII/2) completely failed to interact with U6 snRNA, whereas the stem I deletion derivative (SP6-U4ΔstemI) only reduced the U4-U6 interaction. Perhaps this finding points to differential functions of stem I and stem II, and that these regions may be involved not only in RNA-RNA base pairing. Anti-sense oligonucleotide binding experiments recently also led to the conclusion that not all of the base pairing region of U4 snRNA needs to be intact for the U4-U6 interaction (10).

In contrast to the stem I and stem II regions, the 5′ stem-loop region of U4 snRNA is not essential for U4-U6 interaction. The result that a deletion of this region enhances the U4-U6 interaction, suggests a destabilizing function of the 5′ stem-loop. Previous studies have provided evidence that the U4-U6 interaction weakens during splicing (4,8,9). The failure of the 5′ stem-loop deletion derivative (SP6-U4Δ5′ stem-loop) to assemble into spliceosomes strongly suggests that the 5′ stem-loop structure functions subsequent to the U4-U6 interaction. Potential functions include mediating the interaction between the U4/U6 and U5 snRNPs during the U4/U5/U6 multi-snRNP formation or, alternatively, mediating interactions of the U4/U5/U6 multi-snRNP with other spliceosomal components during spliceosome assembly or splicing. Consistent with such a proposed function is the high degree of structural conservation in the 5′ stem-loop region. The RNA sequence is conserved only in a number of positions in the loop region, but not at all within the stem region (11). Finally, in a previous study on the U4/U6 snRNP structure the loop region of the 5′ stem-loop was found accessible to oligonucleotide-directed RNase H cleavage only after phenolization (35), suggesting specific RNA-protein binding in this region. In yeast, a U4-specific protein has recently been identified (36,37) and mapped to the 5′ end of U4 snRNA (38). Furthermore, a recent mutational analysis in yeast showed that the 5′ stem-loop region of *S.cerevisiae* U4 snRNA is required for U4/U5/U6 multi-snRNP assembly (39). Further studies are directed towards analyzing the functions of the 5′ terminal domain of U4 snRNA during spliceosome assembly and pre-mRNA splicing.

ACKNOWLEDGMENTS

We acknowledge the excellent technical assistance of Andrea Hauser, Stephanie Peczynski, Björn Wieland, and Monika Witte. We thank Hannelore Markert for typing the manuscript and Dr. Mike Cross, Thorsten Wolff and Karsten Gröning for critical comments on the manuscript.

REFERENCES

1. Bindereif, A. and Green, M.R. (1990) In: Setlow, J.K. (ed.), Genetic Engineering–Principles and Methods, Vol. 12. Plenum Publishing Corporation, New York, pp. 201–224.
2. Steitz, J.A., Black, D.L., Gerke, V., Parker, K.A., Krämer, A., Frendewey, D. and Keller, W. (1988) In: Birnstiel, M. (ed.), Structure and Function of Major and Minor Small Nuclear Ribonucleoprotein Particles. Springer Verlag, Berlin, pp. 115–154.
3. Bindereif, A. and Green, M.R. (1987) *EMBO J.* **6**, 2415–2424.
4. Cheng, S.-C. and Abelson, J. (1987) *Genes Dev.* **1**, 1014–1027.
5. Konarska, M.M. and Sharp, P.A. (1987) *Cell* **49**, 763–774.
6. Lossky, M., Anderson, G.J., Jackson, S.P. and Beggs, J. (1987) Cell **51**, 1019–1026.
7. Black, D.L. and Pinto, A.L. (1989) *Mol. Cell. Biol.* **9**, 3350–3359.
8. Pikielny, C.W., Rymond, B.C. and Rosbash, M. (1986) *Nature* **324**, 341–345.
9. Lamond, A.I., Konarska, M.M., Grabowski, P.J. and Sharp, P.A. (1988) *Proc. Natl. Acad. Sci. USA* **85**, 411–415.
10. Blencowe, B.J., Sproat, B.S., Ryder, U., Barabino, S. and Lamond, A.I. (1989) *Cell* **59**, 531–539.
11. Guthrie, C. and Patterson, B. (1988) *Annu. Rev. Genet.* **22**, 387–419.
12. Bringmann, P., Appel, B., Rinke, J., Reuter, R., Theissen, H. and Lührmann, R. (1984) *EMBO J.* **3**, 1357–1363.
13. Hashimoto, C. and Steitz, J.A. (1984) *Nucleic Acids Res.* **12**, 3283–3293.
14. Rinke, J., Appel, B., Digweed, M. and Lührmann, R. (1985) *J. Mol. Biol.* 185, 721–731.
15. Bindereif, A., Wolff, T. and Green, M.R. (1990) *EMBO J.* **9**, 251–255.
16. Lührmann, R. (1988) In: Birnstiel, M. (ed.), Structure and Function of Major and Minor Small Nuclear Ribonucleoprotein Particles. Springer Verlag, Berlin, pp. 71–99.
17. Bringmann, P. and Lührmann, R. (1986) *EMBO J.* **5**, 3509–3516.
18. Bach, M., Winkelmann, G. and Lührmann, R. (1989) *Proc. Natl. Acad. Sci. USA* **86**, 6038–6042.
19. Pikielny, C.W., Bindereif, A. and Green, M.R. (1989) *Genes Dev.* 3, 479–487.
20. Bark, C., Weller, P., Zabielski, J. and Pettersson, U. (1986) *Gene* **50**, 333–344.
21. Kunkel, T.A. (1985) *Proc. Natl. Acad. Sci. USA* **82**, 488–492.
22. Zillmann, M., Zapp, M.L. and Berget, S.M. (1988) *Mol. Cell. Biol.* 8, 814–821.
23. Bindereif, A. and Green, M.R. (1986) *Mol. Cell. Biol.* **6**, 2582–2592.
24. Barabino, S.M.L., Sproat, B.S., Ryder, U., Blencowe, B.J. and Lamond, A.I. (1989) *EMBO J.* **8**, 4171–4178.
25. Dignam, D.L., Lebovitz, R.M. and Roeder, R.D. (1983) *Nucleic Acids Res.* **11**, 1475–1489.
26. Krainer, A.R., Maniatis, T., Ruskin, B. and Green, M.R. (1984) *Cell* 36, 993–1005.
27. Ruskin, B., Krainer, A.R., Maniatis, T. and Green, M.R. (1984) *Cell* **38**, 317–331.
28. Konarska, M.M. and Sharp, P.A. (1986) *Cell* **46**, 845–855.
29. Nelson, K.K. and Green, M.R. (1988) *Genes Dev.* **2**, 319–329.
30. Brow, D.A. and Guthrie, C. (1988) *Nature* **334**, 213–218.
31. Mattaj, I.W. and De Robertis, E. (1985) *Cell* **40**, 111–118.
32. Mattaj, I.W. (1986) *Cell* **46**, 905–911.
33. Hamm, J., Kazmaier, M. and Mattaj, I.W. (1987) *EMBO J.* **6**, 3479–3485.
34. Patton, J.R. and Pederson, T. (1988) *Proc. Natl. Acad. Sci. USA* **85**, 747–751.
35. Black, D.L. and Steitz, J.A. (1986) *Cell* **46**, 697–704.
36. Banroques, J. and Abelson, J. (1989) *Mol. Cell. Biol.* **9**, 3710–3719.
37. Petersen-Bjørn, S., Soltyk, A., Beggs, J.D. and Friesen, J.D. (1989) *Mol. Cell. Biol.* **9**, 3698–3709.
38. Xu, Y., Peteren-Bjødrn, S. and Friesen, J.D. (1990) *Mol. Cell. Biol.* 10, 1217–1225.
39. Bordonné, R., Banroques, J., Abelson, J. and Guthrie, C. (1990) *Genes Dev.* **4**, 1185–1196.
40. Kunkel, G.R., Maser, R.L., Calvet, J.P. and Pederson, T. (1986) *Proc. Natl. Acad. Sci. USA* **83**, 8575–8579.